

# Rate constants for the reactions $\text{H} + \text{O}_2 \rightarrow \text{OH} + \text{O}$ and $\text{D} + \text{O}_2 \rightarrow \text{OD} + \text{O}$ over the temperature range 1085–2278 K by the laser photolysis–shock tube technique

Kuan S. Shin and J. V. Michael

Citation: *J. Chem. Phys.* **95**, 262 (1991); doi: 10.1063/1.461483

View online: <http://dx.doi.org/10.1063/1.461483>

View Table of Contents: <http://jcp.aip.org/resource/1/JCPSA6/v95/i1>

Published by the American Institute of Physics.

## Additional information on J. Chem. Phys.

Journal Homepage: <http://jcp.aip.org/>

Journal Information: [http://jcp.aip.org/about/about\\_the\\_journal](http://jcp.aip.org/about/about_the_journal)

Top downloads: [http://jcp.aip.org/features/most\\_downloaded](http://jcp.aip.org/features/most_downloaded)

Information for Authors: <http://jcp.aip.org/authors>

## ADVERTISEMENT

# Instruments for advanced science

### Gas Analysis



- dynamic measurement of reaction gas streams
- catalysis and thermal analysis
- molecular beam studies
- dissolved species probes
- fermentation, environmental and ecological studies

### Surface Science



- UHV TPD
- SIMS
- end point detection in ion beam etch
- elemental imaging - surface mapping

### Plasma Diagnostics



- plasma source characterization
- etch and deposition process
- reaction kinetic studies
- analysis of neutral and radical species

### Vacuum Analysis



- partial pressure measurement and control of process gases
- reactive sputter process control
- vacuum diagnostics
- vacuum coating process monitoring

contact Hiden Analytical for further details

**HIDEN**  
ANALYTICAL

[info@hideninc.com](mailto:info@hideninc.com)  
[www.HidenAnalytical.com](http://www.HidenAnalytical.com)

CLICK to view our product catalogue



# Rate constants for the reactions $\text{H} + \text{O}_2 \rightarrow \text{OH} + \text{O}$ and $\text{D} + \text{O}_2 \rightarrow \text{OD} + \text{O}$ over the temperature range 1085–2278 K by the laser photolysis–shock tube technique

Kuan S. Shin and J. V. Michael

Chemistry Division, Argonne National Laboratory, Argonne, Illinois 60439

(Received 27 February 1991; accepted 27 March 1991)

Rate constants for the reactions (1)  $\text{H} + \text{O}_2 \rightarrow \text{OH} + \text{O}$  and (2)  $\text{D} + \text{O}_2 \rightarrow \text{OD} + \text{O}$  have been measured over the temperature ranges 1103–2055 K and 1085–2278 K, respectively. The experimental method that has been used is the laser photolysis–shock tube technique. This technique utilizes atomic resonance absorption spectrophotometry (ARAS) to monitor H- or D-atom depletion in the presence of a large excess of reactant,  $\text{O}_2$ . The results can be well represented by the Arrhenius expressions  $k_1(T) = (1.15 \pm 0.16) \times 10^{-10} \exp(-6917 \pm 193 \text{ K}/T) \text{ cm}^3 \text{ molecule}^{-1} \text{ s}^{-1}$ , and  $k_2(T) = (1.09 \pm 0.20) \times 10^{-10} \exp(-6937 \pm 247 \text{ K}/T) \text{ cm}^3 \text{ molecule}^{-1} \text{ s}^{-1}$ . Over the experimental temperature range, the present results show that the isotope effect is unity within experimental uncertainty. The Arrhenius equations,  $k_{-1}(T) = (8.75 \pm 1.24) \times 10^{-12} \exp(1121 \pm 193 \text{ K}/T) \text{ cm}^3 \text{ molecule}^{-1} \text{ s}^{-1}$  and  $k_{-2}(T) = (9.73 \pm 1.79) \times 10^{-12} \exp(526 \pm 247 \text{ K}/T) \text{ cm}^3 \text{ molecule}^{-1} \text{ s}^{-1}$ , for the rate constants of the reverse reactions were calculated from the experimentally measured forward rate constants and expressions for the equilibrium constants that have been derived from the JANAF thermochemical database. The theoretical implications of the present results are also discussed.

## I. INTRODUCTION

The reaction between hydrogen atoms and oxygen molecules,



is one of the most important elementary reactions in gas-phase combustion. Not only is it important in the oxidation of  $\text{H}_2$ ,<sup>1</sup> but it also occurs in the oxidation mechanism of all hydrocarbons.<sup>2</sup> Baulch *et al.*,<sup>3</sup> Cohen and Westberg,<sup>4</sup> and Warnatz,<sup>5</sup> among others, thoroughly reviewed reaction (1). For several years the most reliable description of the high-temperature rate constant was that by Schott.<sup>6</sup> However, Frank and Just<sup>7</sup> questioned the negative  $T$  dependence in the  $A$  factor and reported about a factor of 2 higher rate constant at 2500 K than implied by Schott's expression. Because of its acknowledged importance, the reaction has again been studied by four groups in the past three years.<sup>8–12</sup> These very recent high-temperature experimental data agree with one another below about 2000 K; however, above 2000 K the spread in the values increases to about a factor of 2 as temperature increases to 2500 K.

For the isotopic modification of reaction (1),



only four studies have reported values for the rate constant, and these are derived from chemically modeling the complex  $\text{D}_2$  oxidation mechanism.<sup>13–16</sup> There are no previous direct studies of the rate behavior for reaction (2). Kurzius and Boudart<sup>13</sup> estimated the rate constant from explosion limit studies between 800 and 1000 K, and Appel and Appleton<sup>14</sup> reported shock-tube results for the rate constant from  $\text{D}_2$  oxidation studies between 1700 and 3100 K. The isotope effect was measured by Chiang and Skinner<sup>15</sup> and they reported a larger isotope effect (a factor of 4.5 at 1300 K) than

one would normally expect for this type of reaction. However, Pamidimukkala and Skinner<sup>16</sup> later amended this value downward to 1.4 at 1500 K.

There has also been extensive theoretical work on this reaction. Miller computed quasiclassical trajectory values of the  $T$ -dependent rate constants for  $\text{H} + \text{O}_2$  (Ref. 17) and its deuterated analog.<sup>18</sup> Troe and co-workers performed statistical adiabatic channel model calculations,<sup>19</sup> Rai and Truhlar used variational transition-state theory,<sup>20</sup> Clary and Werner performed quantum scattering calculations,<sup>21</sup> Graff and Wagner studied the fine-structure effects and long-range forces in the potential-energy surface and estimated rate constants with the ACIOSA (adiabatic capture infinite-order sudden approximation) method,<sup>22</sup> Varandas and co-workers applied a double many-body expansion (DMBE) method with subsequent quasiclassical trajectory calculations,<sup>23</sup> and Davidsson and Nyman developed a so-called extended Langevin model.<sup>24</sup> The issue raised in the trajectory calculations of Miller<sup>17,18</sup> was whether dynamical recrossing effects are dictating reactivity. In general, he and others<sup>23</sup> have suggested that recrossing increases with increasing temperature, thereby giving a negative preexponential factor dependence in the rate constant for reaction (1). The existence of such an effect is an apparent point of reference for the extensive theoretical work on this reaction.

The motivation for the present investigation is to measure the rate constants for  $\text{H} + \text{O}_2 \rightarrow \text{OH} + \text{O}$  and  $\text{D} + \text{O}_2 \rightarrow \text{OD} + \text{O}$  with the same laser photolysis–shock tube technique (LP-ST), thereby determining the isotope effect at high temperature. Use of the excimer laser-photolysis method allows experiments to be performed at somewhat higher temperatures than in the previous flash photolysis–shock tube investigation.<sup>10</sup> This is important since the experimental discrepancies appear above  $\sim 2000$  K. Also, the

measurement of the isotope effect may have implications regarding the question of dynamical recrossing.

## EXPERIMENT

The present experiments were performed with the laser photolysis-shock tube (LP-ST) technique.<sup>25,26</sup> This is a special case of the more general flash photolysis-shock tube (FP-ST) technique.<sup>10,27,28</sup> The method and the apparatus currently being used have been previously described,<sup>29-31</sup> and therefore, only a brief description of the system, along with those features unique to the current experimental procedures, will be presented here.

**Apparatus.** A schematic diagram of the LP-ST apparatus is shown in Fig. 1. The apparatus consists of a 7 m (4 in o.d.) 304 stainless-steel tube separated from the He driver chamber by a 4 mil unscored 1100-H18 aluminum diaphragm. The tube was routinely pumped between experiments to  $<10^{-8}$  Torr by an Edwards Vacuum Products model CR100P packaged pumping system. The velocity of the shock wave was measured with eight equally spaced pressure transducers (PCB Piezotronics, Inc., model 113A2) mounted along the end portion of the shock tube, and temperature and density in the reflected shock-wave regime were calculated from this velocity. This procedure has been given previously, and corrections for boundary-layer perturbation were applied.<sup>31,32</sup> Both the 4094C Nicolet digital oscilloscope and the Questek 2000 excimer laser were triggered by delayed pulses that derive from the last velocity gauge signal.

**Laser Photolysis.** The 193.3 nm radiation was produced by a Questek 2000 excimer laser operated in the ArF mode. The beam was directed by two reflectors, and entered the shock tube through a suprasil grade quartz window that was mounted flush to the end plate. The photometer system was radially located at the distance of 6 cm from the end plate.  $\text{MgF}_2$  components were used in the photometer optics. The

resonance lamp beam was detected by an EMR G14 solar blind photomultiplier tube. The photolysis beam at the photometer position was varied from  $1.5$  to  $6 \times 10^{16}$  photons  $\text{cm}^{-2}$ , so that initial H- or D-atom concentration was always less than  $\sim 1 \times 10^{12}$  atoms  $\text{cm}^{-3}$  in the various mixtures. At this concentration level, secondary reactions of H or D atoms with other species are negligible during the time of the experimental observations. In the present studies, H atoms were produced by the photodissociation of either  $\text{H}_2\text{O}$  or  $\text{NH}_3$ , and  $\text{D}_2\text{O}$  was used as the source molecule for the D atom. On photodecomposition, these species gave easily measurable concentrations of atoms in the reflected shock regime.

**Detection by Atomic Absorption.** The technique used for the detection of the transient atomic species is atomic resonance absorption spectroscopy (ARAS).<sup>33</sup> For H atoms, the photometer configuration has been discussed in detail.<sup>34</sup> Unreversed H-atom Lyman- $\alpha$  ( $\text{Ly}_{\alpha\text{H}}$ ) was produced by a 2450 MHz microwave discharge in a 1.7 Torr flow of prepurified He. This transition at 121.6 nm was further spectrally isolated by placing a gas filter section<sup>35</sup> that contains 3 cm of dry air at atmospheric pressure in front of the solar blind photomultiplier. There was always some radiation that is not  $\text{Ly}_{\alpha\text{H}}$ , and it was necessary to determine the fraction of this spectral impurity. Hence, an H-atom filter section was placed in front of the resonance lamp.<sup>36</sup> This filter section is simply a fast discharge-flow system operating with  $\sim 0.2$  Torr of  $\text{H}_2$ . With the microwave discharge operating, sufficient H-atom concentration was produced in the optical path to nearly remove all of  $\text{Ly}_{\alpha\text{H}}$  radiation. The measurement of the fraction of light that was resonance radiation was routinely made before each kinetic experiment. The configuration used for D-atom studies was exactly the same as that for the H atom except that a flowing premixture of 5–10 ppm of  $\text{D}_2$  in He was used as the source of  $\text{Ly}_{\alpha\text{D}}$ . The light coming from the lamp contains not only the desired  $\text{Ly}_{\alpha\text{D}}$  but also  $\text{Ly}_{\alpha\text{H}}$ . Hence, it was necessary to remove  $\text{Ly}_{\alpha\text{H}}$  by

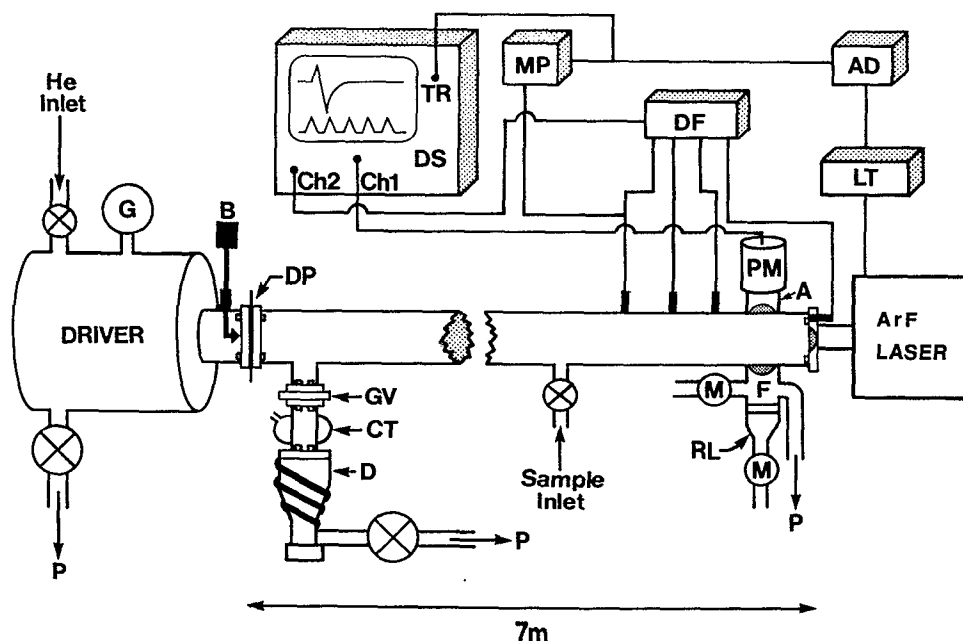
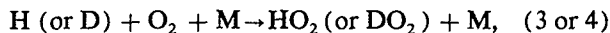
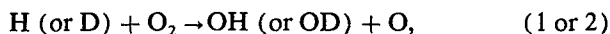


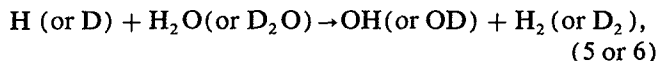
FIG. 1. Schematic diagram of the apparatus. A, gas and crystal window filter. AD, delayed pulse generator. B, breaker. CT, liquid-nitrogen baffle. D, oil diffusion pump. DF, differentiator. DP, diaphragm. DS, digital oscilloscope. F, atomic filter. G, bourdon gauge. GV, gate valve. LT, laser trigger. M, microwave power supply. MP, master pulse generator. P, rotary pump. PM, photomultiplier. RL, resonance lamp. TR, trigger pulse. Solid plugs on shock tube and end-plate are pressure transducers.

operating the H-atom filter section during the kinetics experiments.

**Kinetics Analysis.** After their formation by laser photolysis, H or D atoms are depleted by the following reactions:



and



or



In this study,  $[\text{M}]$  is taken to be the overall concentration (density), which includes Ar,  $\text{O}_2$ , and  $\text{H}_2\text{O}$  (or  $\text{D}_2\text{O}$ ), or  $\text{NH}_3$ . The concentration of Ar,  $\text{O}_2$ , and  $\text{H}_2\text{O}$  (or  $\text{D}_2\text{O}$ ), or  $\text{NH}_3$  were always maintained in large excess over  $[\text{H}]$  (or  $[\text{D}]$ ). Therefore, each of these reactions follows pseudo-first-order kinetics. Consequently,

$$d[\text{H (or D)}]/dt = -k_{\text{obs}}[\text{H (or D)}], \quad (8)$$

where

$$k_{\text{obs}} = k_1[\text{O}_2] + k_3[\text{O}_2][\text{M}] + k_5[\text{H}_2\text{O}], \quad (9)$$

or, in the deuterium substituted case,

$$k_{\text{obs}} = k_2[\text{O}_2] + k_4[\text{O}_2][\text{M}] + k_6[\text{D}_2\text{O}], \quad (10)$$

For the  $\text{H} + \text{O}_2$  reaction studies with  $\text{NH}_3$  as the source molecule,

$$k_{\text{obs}} = k_1[\text{O}_2] + k_3[\text{O}_2][\text{M}] + k_7[\text{NH}_3]. \quad (11)$$

In the range of H- or D-atom concentrations used in these experiments, Beer's law is always valid.<sup>34</sup> Therefore, atom concentration is equal to  $(\text{ABS})_t/\sigma l$  where  $(\text{ABS})_t$  is defined as  $-\ln(I_t/I_0)$  ( $I_t$  and  $I_0$  refer to time-dependent and incident photometric intensities, respectively,  $\sigma$  is the effective atom cross section, and  $l$  is the absorption path length). Thus,

$$\ln(\text{ABS})_t = -k_{\text{obs}}(t) + C, \quad (12)$$

and a plot of  $\ln(\text{ABS})_t$  vs time has a slope equal to  $-k_{\text{obs}}$ . Figure 2 shows a typical data record and the corresponding first-order plot of  $\ln(\text{ABS})_t$  against time. All H- or D-atom decays obeyed first-order kinetics with no evidence of complex kinetic behavior under the conditions of the present experiments. This observation was further supported by the results from computer simulations which took secondary reactions into account. The rate constants for reactions 3, 5, 6, or 7 have been directly measured in the appropriate temperature range in separate experiments ( $k_3$ : Refs. 10 and 37;  $k_5$ : Ref. 38;  $k_6$ : Ref. 30;  $k_7$ : Ref. 39). Even though reactions (3) and (4) were included in the analysis ( $k_3$  assumed to be equal to  $k_4$ ), they were negligible. Therefore, the sum of contributions from reactions 5, 6, and/or 7 was calculated for each experiment and was subtracted from  $k_{\text{obs}}$ . This correction was usually less than 10% of  $k_{\text{obs}}$  except at the highest temperature where it reached  $\sim 25\%$ .

**Gases.** Ar diluent for the experimental mixtures was obtained from MG Industries (scientific grade, 99.9999%) and was used without further purification. He, used as re-

ceived as the driver gas and also in the resonance lamp and atomic filter section, was ultrahigh purity grade (99.995%) and was obtained from Airco Industrial Gases. In the atomic filter section,  $\text{H}_2$  from Airco Industrial Gases (prepurified, 99.995%) was used as received.  $\text{D}_2$ , supplied by Air Products and Chemicals, Inc., was research grade (99.99%).  $\text{O}_2$  from MG Industries (scientific grade, 99.999%) was used without further purification. All of the source molecules,  $\text{H}_2\text{O}$ ,  $\text{D}_2\text{O}$ , and  $\text{NH}_3$ , were bulb-to-bulb distilled in a greaseless, all-glass, high-vacuum gas-handling system: the middle one-third fractions were retained.  $\text{D}_2\text{O}$  was obtained from Mallinckrodt Chemical Works and isotopic analysis showed it to contain 96.4%  $\text{D}_2\text{O}$ , 3.4%  $\text{HDO}$ , and 0.2%  $\text{H}_2\text{O}$ .

## RESULTS

Experiments were performed over the temperature range 1085–2278 K, under the conditions shown in Tables I and II. The thermodynamic state of the hot gas was determined from the measured Mach number, initial pressure, and temperature. Corrections for boundary-layer effects were applied, as described previously.<sup>31,32</sup> The resultant density,  $\rho_5$ , and temperature,  $T_5$ , in the reflected region are shown in the tables. Estimates of the accuracy of these quantities rest on the accuracy of the Mach number ( $\sim \pm 0.5\%$ – $1\%$ ) which gives  $\sim \pm 2\%$ – $4\%$  and  $\sim \pm 1\%$ – $2\%$  uncertainties in  $\rho_5$  and  $T_5$ , respectively. In addition, the absolute accuracy of decay constant determination is  $\sim \pm 10\%$ . The possibility of adsorption and/or desorption of  $\text{H}_2\text{O}$  or  $\text{D}_2\text{O}$  on the walls of the shock tube and gas-handling system was discussed in detail in previous work.<sup>30,38</sup> All of these uncertainties combine to give the scatter shown in Figs. 3 and 4 where the data in Tables I and II are plotted in Arrhenius form. In the determination of the rate constants for reaction (1), both  $\text{H}_2\text{O}$  and  $\text{NH}_3$  were used as source molecules. Accordingly, the correction to  $k_{\text{obs}}$ , yielding the decay constants due to reaction (1) alone, was different in the two cases. The corrected values for  $k_1$  are listed in Table I. The values with  $\text{H}_2\text{O}$  were  $\sim \pm 20\%$  higher than with  $\text{NH}_3$  over the experimental temperature range; however, when the scatter of each set was determined at the  $\pm 1\sigma$  level, it was found that the two sets overlapped significantly and were therefore not statistically distinguishable. We therefore combined the two sets and analyzed them together.

The corrected results for  $\text{H} + \text{O}_2 \rightarrow \text{OH} + \text{O}$  (1103–2055 K) and  $\text{D} + \text{O}_2 \rightarrow \text{OD} + \text{O}$  (1085–2278 K) are given in Tables I and II and are plotted in Arrhenius form in Figs. 3 and 4. The lines shown in figures are given by the equations

$$k_1 = (1.15 \pm 0.16) \times 10^{-10} \exp(-6917 \pm 193 \text{ K}/T) \quad (13)$$

and

$$k_2 = (1.09 \pm 0.20) \times 10^{-10} \exp(-6937 \pm 247 \text{ K}/T) \quad (14)$$

in  $\text{cm}^3 \text{ molecule}^{-1} \text{ s}^{-1}$ , where the errors are given at the one-standard-deviation level. The individual points deviate from the line expressed by Eq. (13) by  $\pm 27\%$ , whereas the deviation of the points from Eq. (14) is  $\pm 24\%$  with both values determined at the one-standard-deviation level. It is

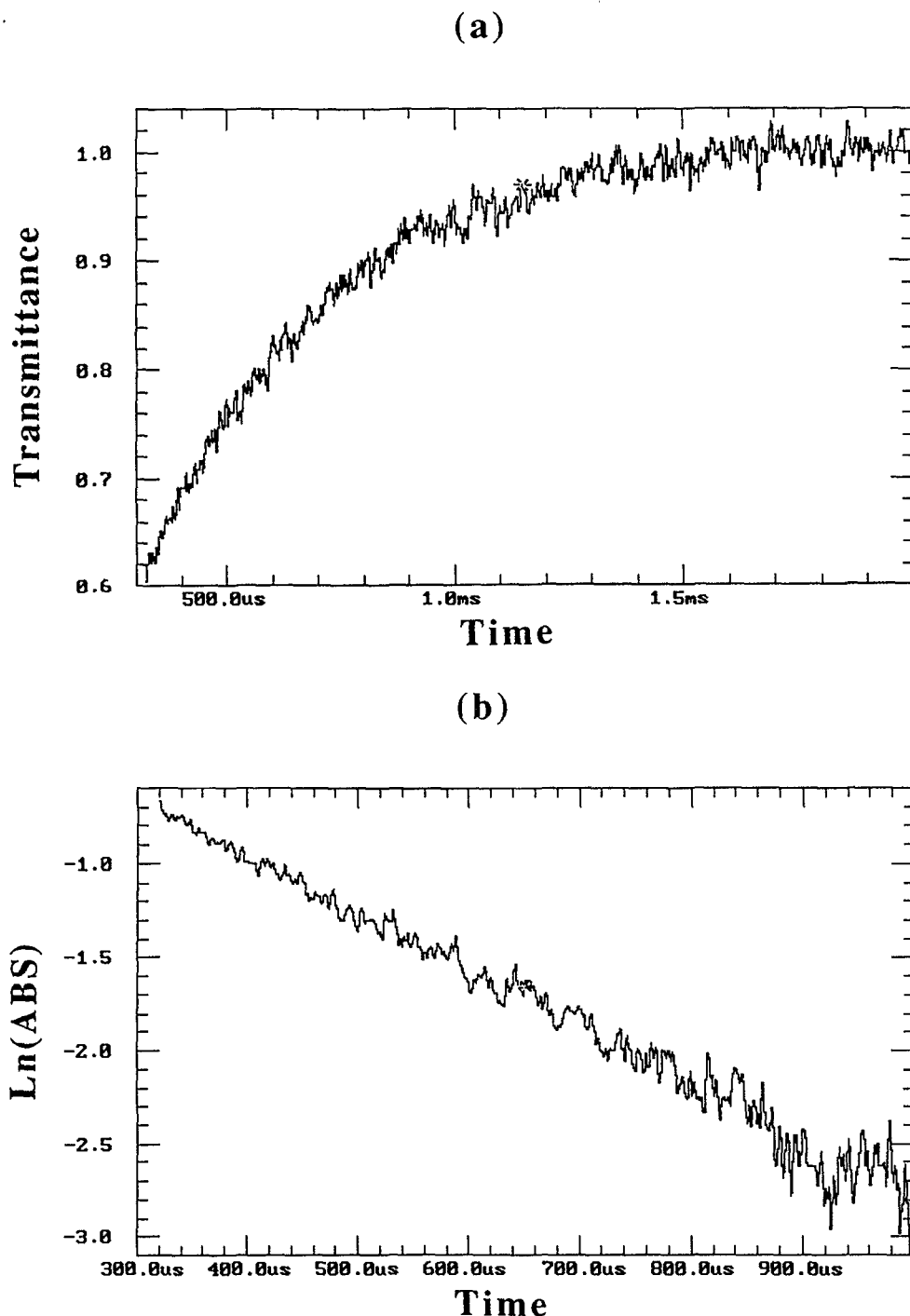


FIG. 2. (a) H-atom transmittance as a function of time after laser photolysis. (b) First-order plot of  $\ln(\text{ABS})$ , against time that is obtained from the record in panel (a);  $k_{1st} = 3012 \text{ s}^{-1}$  in an  $\text{H} + \text{O}_2$  experiment where  $[\text{O}_2] = 1.58 \times 10^{15} \text{ cm}^{-3}$  at 1697 K giving  $k_{\text{H} + \text{O}_2}(1697 \text{ K}) = 1.81 \times 10^{-12} \text{ cm}^3 \text{ molecule}^{-1} \text{ s}^{-1}$ .

obvious by inspection that, within experimental error, there is not a significant isotope effect.

The reverse rate constants,  $k_{-1}$  and  $k_{-2}$  for  $\text{O} + \text{OH} \rightarrow \text{H} + \text{O}_2$  and  $\text{O} + \text{OD} \rightarrow \text{D} + \text{O}_2$ , respectively, can be derived from Eqs. (13) and (14) and corresponding equilibrium constants. The equilibrium constant values were calculated from data in the JANAF tables<sup>40</sup> between 1000 and 2300 K, and the derived linear least-squares expressions are

$$K_1 = (13.19 \pm 0.18) \exp(-8038 \pm 21 \text{ K}/T) \quad (15)$$

and

$$K_2 = (11.24 \pm 0.08) \exp(-7463 \pm 12 \text{ K}/T). \quad (16)$$

Equations (15) and (16) are accurate to within about  $\pm 1\%$  over their respective temperature ranges. The reverse rate constants can now be determined from each value in Table I and II, and analysis of the results gives the equations

$$k_{-1} = (8.75 \pm 1.24) \times 10^{-12} \exp(1121 \pm 193 \text{ K}/T) \quad (17)$$

and

$$k_{-2} = (9.73 \pm 1.79) \times 10^{-12} \exp(526 \pm 247 \text{ K}/T) \quad (18)$$

TABLE I. Rate data for the reaction  $\text{H} + \text{O}_2 \rightarrow \text{OH} + \text{O}$ .

$P_1$ (Torr)	$M_1^a$	$k_{1st} \text{ s}^{-1}{}^b$	$\rho_5 (10^{18} \text{ cm}^{-3})^c$	$T_5$ (K) <sup>c</sup>	$k_1 (10^{-13} \text{ cm}^3 \text{ s}^{-1})^d$
$X_{\text{O}_2} = 7.000 \times 10^{-4}$			$X_{\text{H}_2\text{O}} = 4.250 \times 10^{-4}$		
10.93	2.851	6 092	2.357	1 993	28.37
10.88	2.449	2 622	2.045	1 507	16.90
10.90	2.884	10 805	2.372	2 036	55.43
10.91	2.525	3 569	2.113	1 593	22.04
10.98	2.793	5 850	2.329	1 919	29.03
10.91	2.898	8 112	2.383	2 055	38.46
10.96	2.779	9 648	2.314	1 900	53.09
10.93	2.901	7 946	2.390	2 059	37.23
$X_{\text{O}_2} = 1.175 \times 10^{-3}$			$X_{\text{H}_2\text{O}} = 4.125 \times 10^{-4}$		
10.90	2.433	2 934	2.021	1 498	11.52
10.98	2.574	4 029	2.152	1 660	14.29
10.79	2.718	6 473	2.222	1 836	21.71
10.94	2.775	16 735	2.285	1 913	58.38
10.85	2.742	6 708	2.251	1 866	21.95
10.92	2.659	7 366	2.205	1 762	26.03
10.85	2.637	5 538	2.175	1 736	19.48
10.95	2.647	9 941	2.202	1 748	36.13
$X_{\text{O}_2} = 1.388 \times 10^{-3}$			$X_{\text{H}_2\text{O}} = 1.313 \times 10^{-3}$		
10.96	2.448	4 135	2.041	1 518	12.35
10.90	2.273	1 711	1.879	1 291	5.89
10.91	2.332	2 897	1.936	1 385	9.64
10.97	2.392	3 424	2.001	1 451	10.71
10.84	2.425	4 255	1.999	1 492	13.35
10.90	2.621	7 906	2.176	1 714	20.96
10.99	2.600	7 322	2.170	1 695	19.46
10.94	2.437	4 450	2.028	1 506	13.68
$X_{\text{O}_2} = 2.513 \times 10^{-3}$			$X_{\text{H}_2\text{O}} = 1.838 \times 10^{-3}$		
10.87	2.233	3 501	1.846	1 274	7.05
10.94	2.332	5 578	1.945	1 384	10.50
10.97	2.329	6 064	1.947	1 380	11.50
10.98	2.245	2 386	1.870	1 292	4.52
10.88	2.151	1 531	1.755	1 200	3.14
10.96	2.156	2 894	1.773	1 205	6.15
10.90	2.183	2 504	1.802	1 224	5.15
10.92	2.060	1 531	1.678	1 103	3.42
10.91	2.331	2 959	1.939	1 382	5.18
10.92	2.397	5 623	2.006	1 449	9.89
$X_{\text{O}_2} = 7.000 \times 10^{-4}$			$X_{\text{H}_2\text{O}} = 4.250 \times 10^{-4}$		
15.92	2.303	2 236	2.795	1 353	10.71
15.94	2.407	2 507	2.917	1 468	11.05
15.99	2.588	3 892	3.129	1 671	14.84
16.00	2.818	17 028	3.355	1 947	64.99
15.93	2.771	7 836	3.298	1 890	27.63
15.83	2.895	16 813	3.386	2 046	60.96
15.87	2.786	8 936	3.299	1 909	31.99
15.86	2.803	11 503	3.313	1 930	42.46
$X_{\text{O}_2} = 1.175 \times 10^{-3}$			$X_{\text{H}_2\text{O}} = 4.125 \times 10^{-4}$		
15.99	2.561	5 669	3.112	1 633	13.97
15.85	2.716	13 360	3.231	1 822	32.19
15.89	2.434	4 419	2.941	1 497	11.90
15.99	2.167	1 616	2.618	1 219	4.96
15.92	2.324	2 931	2.813	1 378	8.33
15.94	2.444	3 647	2.961	1 507	9.56
15.91	2.545	5 591	3.079	1 615	14.03
15.91	2.562	7 377	3.098	1 635	18.72
$X_{\text{O}_2} = 1.388 \times 10^{-3}$			$X_{\text{H}_2\text{O}} = 1.313 \times 10^{-3}$		
15.79	2.400	4 612	2.885	1 457	9.79
15.91	2.227	2 292	2.688	1 277	5.47
15.93	2.582	8 848	3.106	1 666	16.15

TABLE 1. (continued).

$P_1$ (Torr)	$M_s^{a)}$	$k_{1st} \text{ s}^{-1b)}$	$\rho_5 (10^{18} \text{ cm}^{-3})^{c)}$	$T_5$ (K)	$k_1 (10^{-13} \text{ cm}^2 \text{ s}^{-1})^{d)}$
15.98	2.404	4 383	2.926	1 462	9.03
15.93	2.257	2 867	2.732	1 308	6.76
15.90	2.244	3 018	2.710	1 295	7.28
$X_{\text{O}_2} = 2.513 \times 10^{-3}$		$X_{\text{H}_2\text{O}} = 1.838 \times 10^{-3}$			
15.88	2.199	4 053	2.659	1 244	5.59
15.89	2.363	8 814	2.873	1 411	11.11
15.86	2.171	2 912	2.636	1 208	3.99
15.85	2.212	3 291	2.681	1 252	4.39
15.78	2.086	2 272	2.483	1 134	3.35
15.89	2.105	2 259	2.528	1 152	3.24
15.86	2.075	2 287	2.471	1 127	3.40
15.90	2.165	2 630	2.606	1 214	3.60
$X_{\text{O}_2} = 7.250 \times 10^{-4}$		$X_{\text{NH}_3} = 2.276 \times 10^{-5}$			
10.94	2.661	3 738	2.209	1 766	22.24
10.97	2.587	3 088	2.152	1 684	18.88
10.88	2.811	5 743	2.295	1 962	32.84
10.74	2.868	4 798	2.302	2 037	26.82
10.88	2.849	4 874	2.351	1 984	26.84
10.73	2.572	2 619	2.114	1 649	16.25
10.96	2.434	2 186	2.046	1 490	14.19
10.94	2.419	2 088	2.022	1 479	13.72
10.95	2.609	3 012	2.179	1 697	18.13
10.81	2.511	2 158	2.074	1 582	13.65
$X_{\text{O}_2} = 1.563 \times 10^{-3}$		$X_{\text{NH}_3} = 3.107 \times 10^{-5}$			
10.95	2.388	3 127	1.992	1 448	9.70
10.94	2.725	10 093	2.250	1 852	27.81
10.95	2.500	3 743	2.080	1 579	11.04
10.89	2.401	2 971	1.985	1 467	9.22
10.95	2.324	2 168	1.927	1 382	6.91
10.86	2.261	1 782	1.860	1 311	5.89
10.93	2.271	2 479	1.875	1 326	8.21
10.92	2.410	2 673	2.005	1 472	8.16
10.90	2.439	2 924	2.040	1 494	8.79
10.97	2.735	8 754	2.286	1 845	23.63
$X_{\text{O}_2} = 2.513 \times 10^{-3}$		$X_{\text{NH}_3} = 2.144 \times 10^{-5}$			
10.89	2.502	8 917	2.072	1 581	16.86
10.93	2.376	4 131	1.972	1 439	8.13
10.94	2.340	3 006	1.941	1 399	5.97
10.89	2.243	1 810	1.868	1 279	3.69
10.90	2.068	1 003	1.687	1 109	2.24
10.95	2.249	2 028	1.877	1 289	4.13
10.92	2.197	1 890	1.822	1 236	3.98
10.89	2.179	1 697	1.793	1 222	3.62
10.92	2.153	1 389	1.772	1 196	2.98
10.90	2.334	3 329	1.942	1 383	6.63
$X_{\text{O}_2} = 7.250 \times 10^{-4}$		$X_{\text{NH}_3} = 2.276 \times 10^{-5}$			
15.80	2.369	2 092	2.845	1 427	9.64
15.96	2.424	2 496	2.939	1 486	11.13
15.93	2.671	4 805	3.201	1 769	19.54
15.94	2.753	5 349	3.282	1 869	21.04
15.98	2.834	7 481	3.364	1 970	28.92
15.88	2.551	3 191	3.067	1 629	13.51
15.71	2.597	5 395	3.082	1 682	23.19
15.98	2.658	4 261	3.198	1 754	17.25
15.78	2.561	3 821	3.058	1 640	16.37
15.81	2.500	2 558	2.998	1 570	11.04
$X_{\text{O}_2} = 1.563 \times 10^{-3}$		$X_{\text{NH}_3} = 3.107 \times 10^{-5}$			
15.77	2.348	3 924	2.816	1 404	8.56
15.86	2.316	3 397	2.792	1 370	7.45
15.93	2.495	5 583	3.037	1 553	11.26
15.83	2.595	6 097	3.126	1 667	11.83

TABLE I. (continued).

$P_1$ (Torr)	$M_s^a$	$k_{1st} \text{ s}^{-1b}$	$\rho_5 (10^{18} \text{ cm}^{-3})^c$	$T_5$ (K)	$k_1 (10^{-13} \text{ cm}^2 \text{ s}^{-1})^d$
15.85	2.728	19 880	3.253	1 831	38.20
15.99	2.517	7 210	3.064	1 584	14.52
15.91	2.629	8 200	3.156	1 718	15.90
16.00	2.437	4 675	2.964	1 500	9.64
15.97	2.176	1 569	2.627	1 228	3.57
15.98	2.538	7 051	3.085	1 608	14.05
$X_{\text{O}_2} = 2.513 \times 10^{-3}$			$X_{\text{NH}_3} = 2.144 \times 10^{-5}$		
15.86	2.261	3 285	2.723	1 312	4.58
15.91	2.129	1 764	2.552	1 181	2.56
16.00	2.049	1 359	2.450	1 104	2.03
15.84	2.148	1 523	2.560	1 204	2.17
15.92	2.107	2 091	2.515	1 163	3.12
15.97	2.170	2 245	2.611	1 225	3.22
15.90	2.188	2 077	2.634	1 239	2.94
15.87	2.211	2 574	2.659	1 261	3.64
15.88	2.395	5 749	2.885	1 458	7.66
15.92	2.229	3 130	2.683	1 284	4.43

<sup>a</sup>The errors in Mach number were typically about  $\pm 0.5\%$  at the one-standard-deviation level.

<sup>b</sup>The errors in  $k_{1st}$  ranged from about  $\pm 4\%$  to  $\pm 10\%$ , at the two-standard-deviation level.

<sup>c</sup>Quantities with the subscript 5 refer to the thermodynamic state of the gas in the reflected region.

<sup>d</sup>This is the corrected bimolecular rate constant according to Eqs. (9) or (11) (see text).

<sup>e</sup> $X_i$  denotes the mole fraction of species,  $i$ .

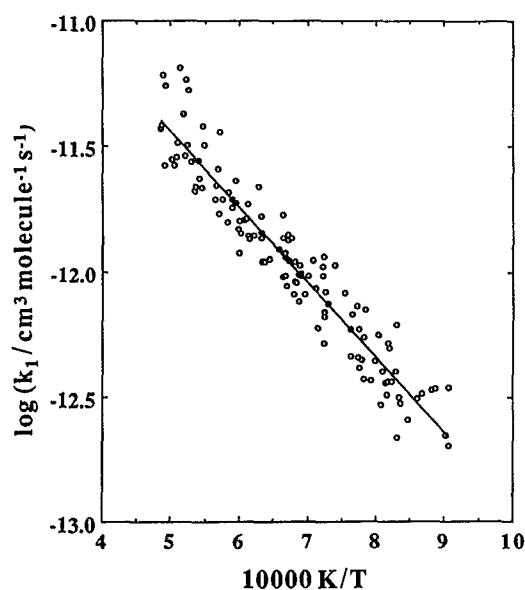
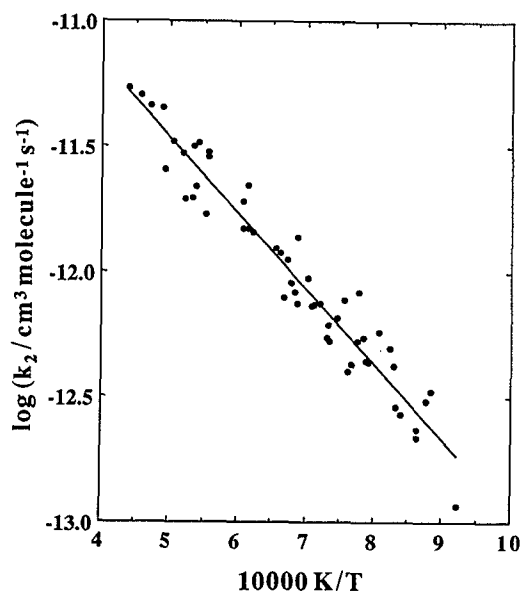
TABLE II. Rate data for the reaction  $\text{D} + \text{O}_2 \rightarrow \text{OD} + \text{O}$ .

$P_1$ (Torr)	$M_s^a$	$k_{1st} (\text{s}^{-1})^b$	$\rho_5 (10^{18} \text{ cm}^{-3})^c$	$T_5$ (K) <sup>c</sup>	$k_1 (10^{-13} \text{ cm}^3 \text{ s}^{-1})^d$
$X_{\text{O}_2} = 8.125 \times 10^{-4}$			$X_{\text{D}_2\text{O}} = 5.625 \times 10^{-4}$		
10.85	2.552	4 291	2.117	1 629	22.20
10.91	2.758	4 875	2.283	1 880	19.79
10.94	2.997	12 919	2.453	2 187	50.40
10.88	2.740	5 165	2.264	1 857	22.03
10.89	2.693	6 375	2.232	1 799	30.11
10.91	2.890	10 659	2.371	2 050	44.93
10.91	3.057	14 423	2.474	2 278	54.22
10.90	2.731	7 100	2.261	1 845	32.81
10.92	2.794	6 962	2.310	1 926	29.67
10.92	2.939	11 368	2.397	2 123	45.94
10.91	2.869	6 779	2.350	2 030	25.63
10.97	2.831	7 963	2.337	1 980	33.28
$X_{\text{O}_2} = 1.313 \times 10^{-3}$			$X_{\text{D}_2\text{O}} = 1.300 \times 10^{-3}$		
10.98	2.192	1 514	1.817	1 239	5.77
10.97	2.398	2 679	2.001	1 462	8.32
10.99	2.526	5 009	2.112	1 608	14.50
10.90	2.561	6 469	2.122	1 648	19.05
10.92	2.419	3 499	2.010	1 486	11.16
$X_{\text{O}_2} = 2.819 \times 10^{-3}$			$X_{\text{D}_2\text{O}} = 1.794 \times 10^{-3}$		
10.87	2.338	4 573	1.939	1 389	7.48
10.83	2.547	10 329	2.103	1 630	14.88
10.91	2.433	5 341	2.023	1 498	7.90
10.84	2.370	5 813	1.962	1 423	9.47
10.88	2.394	4 847	1.984	1 455	7.46
10.94	2.272	2 471	1.896	1 315	4.01
10.96	2.319	3 802	1.944	1 365	6.15
10.95	2.259	2 551	1.879	1 305	4.23
10.94	2.095	1 588	1.714	1 141	3.03
10.91	2.151	1 511	1.772	1 191	2.70
$X_{\text{O}_2} = 8.125 \times 10^{-4}$			$X_{\text{D}_2\text{O}} = 5.625 \times 10^{-4}$		
15.88	2.438	3 654	2.953	1 457	13.85



TABLE II. (continued).

$P_1$ (Torr)	$M_1$ <sup>a</sup>	$k_{1st}$ ( $\text{s}^{-1}$ ) <sup>b</sup>	$\rho_5$ ( $10^{18} \text{ cm}^{-3}$ ) <sup>c</sup>	$T_5$ (K) <sup>c</sup>	$k_1$ ( $10^{-13} \text{ cm}^3 \text{ s}^{-1}$ ) <sup>d</sup>
15.90	2.574	4 519	3.109	1 649	14.87
15.88	2.798	7 232	3.325	1 916	19.49
15.82	2.705	8 925	3.225	1 802	28.92
15.88	2.711	5 870	3.243	1 810	17.00
15.90	2.763	10 278	3.297	1 873	31.96
15.93	2.451	3 296	2.978	1 510	11.89
15.88	2.228	1 326	2.691	1 275	5.48
15.82	2.468	3 468	2.976	1 528	12.47
15.88	2.240	1 973	2.707	1 287	8.35
$X_{\text{O}_2} = 1.313 \times 10^{-3}$			$X_{\text{D}_2\text{O}} = 1.300 \times 10^{-3}$		
15.87	2.285	2 758	2.750	1 341	6.57
15.93	2.346	3 295	2.837	1 405	7.37
15.97	2.347	3 279	2.836	1 411	7.29
15.94	2.263	3 102	2.724	1 322	7.70
15.89	2.100	908	2.493	1 160	2.35
15.89	2.155	1 857	2.571	1 214	4.95
15.91	2.408	4 236	2.899	1 476	9.08
$X_{\text{O}_2} = 2.819 \times 10^{-3}$			$X_{\text{D}_2\text{O}} = 1.794 \times 10^{-3}$		
15.87	2.237	4 467	2.691	1 289	5.30
15.98	2.314	5 009	2.811	1 369	5.47
15.89	2.148	2 380	2.574	1 201	2.89
15.90	2.078	2 529	2.474	1 133	3.33
15.87	2.216	3 662	2.673	1 264	4.34
15.97	2.306	4 799	2.798	1 360	5.26
15.91	2.226	3 757	2.701	1 269	4.40
15.94	2.160	3 379	2.607	1 208	4.19
15.98	2.031	964	2.425	1 085	1.16
15.85	2.110	1 786	2.521	1 160	2.18

<sup>a</sup>The errors in Mach number were typically about  $\pm 0.5\%$  at the one standard deviation level.<sup>b</sup>The errors in  $k_{1st}$  ranged from about  $\pm 4\%$  to  $\pm 10\%$ , at the two standard deviation level.<sup>c</sup>Quantities with the subscript 5 refer to the thermodynamic state of the gas in the reflected region.<sup>d</sup>This is the corrected bimolecular rate constant according to Eq. (10) (see text).<sup>e</sup> $X_i$  denotes the mole fraction of species,  $i$ .FIG. 3. Arrhenius plot of the experimental data for  $\text{H} + \text{O}_2 \rightarrow \text{OH} + \text{O}$ . The solid line is a two-parameter fit of the form  $k = A \exp(-B/T)$  and is given as Eq. (13).FIG. 4. Arrhenius plot of the experimental data for  $\text{D} + \text{O}_2 \rightarrow \text{OD} + \text{O}$ . The solid line is a two-parameter fit of the form  $k = A \exp(-B/T)$  and is given as Eq. (14).

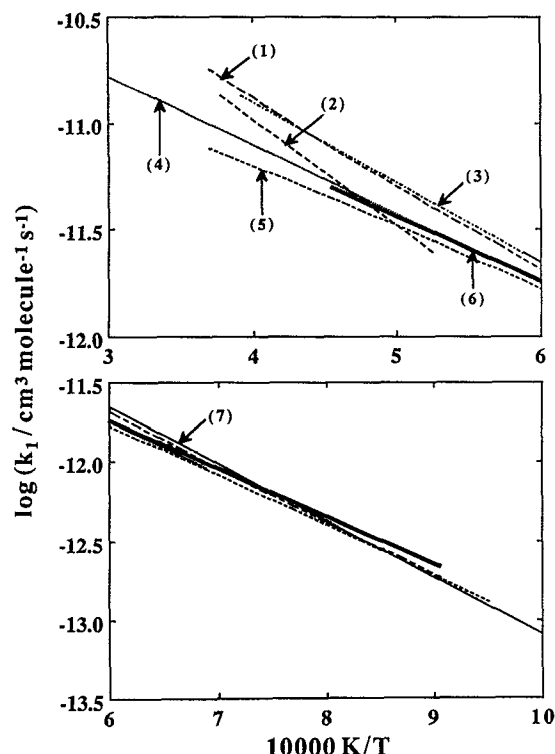


FIG. 5. Comparison of the LP-ST results for  $\text{H} + \text{O}_2 \rightarrow \text{OH} + \text{O}$  to the previous results. (1) Fujii *et al.* (Ref. 9); (2) Fujii and Shin (Ref. 8); (3) Frank and Just (Ref. 7); (4) Masten, Hanson, and Bowman (Ref. 11); (5) Yuan *et al.* (Ref. 12); (6) this work; (7) Pirraglia *et al.* (Ref. 10).

in  $\text{cm}^3 \text{ molecule}^{-1} \text{ s}^{-1}$ , where the errors are given at the one-standard-deviation level.

## DISCUSSION

The result of the present study, Eq. (13), is compared to previous experimental results in Fig. 5, and it is also listed in Table III along with results from previous reviews,<sup>3-5</sup> experimental studies,<sup>6-12,16</sup> and calculations.<sup>17,19</sup> Pirraglia *et al.*<sup>10</sup> measured rate constants for reaction (1) under pseudo-first-order conditions by the flash photolysis-shock tube technique, and they used the same H-atom ARAS detection method as used in the present investigation. For the temperature range, 962–1705 K, they reported

$$k_1 = (2.79 \pm 0.32) \times 10^{-10} \exp(-8119 \pm 139 \text{ K}/T) \quad (19)$$

in  $\text{cm}^3 \text{ molecule}^{-1} \text{ s}^{-1}$ . Comparing Eqs. (13) and (19), the activation energy and preexponential factor are higher by factors of 1.17 and 2.43 in the FP-ST (Ref. 10) than in the present work; however, the two expressions indicate quite good agreement within combined experimental uncertainties in the region of mutual temperature overlap. The recent high-temperature results<sup>8,9,11,12</sup> are summarized in equation form as

TABLE III.  $k = A(T/K)^n \exp(-B/T)$  expressions for  $\text{H} + \text{O}_2 \rightarrow \text{OH} + \text{O}$  and  $\text{D} + \text{O}_2 \rightarrow \text{OD} + \text{O}$ .

$A$ ( $\text{cm}^3 \text{ molecule}^{-1} \text{ s}^{-1}$ )	$n$	$B$ (K)	$T$ range (K)	Reference
Rate constant expressions for $\text{H} + \text{O}_2 \rightarrow \text{OH} + \text{O}$				
$3.70 \times 10^{-10}$	0.0	8449	1700–2500	<sup>a</sup> Baulch <i>et al.</i> (Ref. 3)
$2.77 \times 10^{-7}$	–0.9	8749	300–2500	Cohen and Westberg (Ref. 4)
$2.02 \times 10^{-7}$	–0.91	8305	300–2500	Warnatz (Ref. 5)
$2.02 \times 10^{-7}$	–0.907	8368	1250–2500	<sup>b</sup> Schott (Ref. 6)
$2.00 \times 10^{-10}$	0.0	8101	1000–2500	Pamdimukkala and Skinner (Ref. 16)
$(4.05 \pm 0.55) \times 10^{-10}$	0.0	$8690 \pm 264$	1690–2580	Frank and Just (Ref. 7)
$9.96 \times 10^{-10}$	0.0	11 426	1900–2650	Fujii and Shin (Ref. 8)
$1.66 \times 10^{-17}$	2.0	5172	1100–2700	Fujii <i>et al.</i> (Ref. 9)
$(2.79 \pm 0.32) \times 10^{-10}$	0.0	$8119 \pm 139$	960–1710	Pirraglia <i>et al.</i> (Ref. 10)
$(1.55 \pm 0.07) \times 10^{-10}$	0.0	$7448 \pm 86$	1450–3370	Masten <i>et al.</i> (Ref. 11)
$2.64 \times 10^{-7}$	–0.927	8493	1050–2700	Yuan <i>et al.</i> (Ref. 12)
$(1.15 \pm 0.16) \times 10^{-10}$	0.0	$6917 \pm 193$	1103–2055	This work
$8.52 \times 10^{-8}$	–0.816	8307	250–2500	<sup>c</sup> Miller (Ref. 17)
$2.46 \times 10^{-10}$	0.0	7788	1000–2600	Troe (Ref. 19)
Rate constant expressions for $\text{D} + \text{O}_2 \rightarrow \text{OD} + \text{O}$				
$1.47 \times 10^{-10}$	0.0	7498	800–1000	<sup>b</sup> Kurzius and Boudart (Ref. 13)
$5.20 \times 10^{-10}$	0.0	9934	1700–3100	Appel and Appleton (Ref. 14)
$2.66 \times 10^{-11}$	0.0	7553	925–2200	Chiang and Skinner (Ref. 15)
$9.60 \times 10^{-11}$	0.0	7553	1000–2500	Pamdimukkala and Skinner (Ref. 16)
$(1.09 \pm 0.20) \times 10^{-10}$	0.0	$6937 \pm 247$	1085–2278	This work
$1.35 \times 10^{-8}$	–0.659	7569	250–2500	<sup>c</sup> Miller (Ref. 18)

<sup>a</sup> Review.

<sup>b</sup> Experiment.

<sup>c</sup> Theory.

$$k_1 = 9.96 \times 10^{-10} \exp(-11\,426 \text{ K}/T) \text{ cm}^3 \text{ molecule}^{-1} \text{ s}^{-1} \quad (1900\text{--}2650 \text{ K}) \quad (\text{Ref. 8}), \quad (20)$$

$$k_1 = 1.66 \times 10^{-17} (T/\text{K})^{2.0} \exp(-5172 \text{ K}/T) \text{ cm}^3 \text{ molecule}^{-1} \text{ s}^{-1} \quad (1100\text{--}2700 \text{ K}) \quad (\text{Ref. 9}), \quad (21)$$

$$k_1 = (1.55 \pm 0.07) \times 10^{-10} \exp(-7448 \pm 86 \text{ K}/T) \text{ cm}^3 \text{ molecule}^{-1} \text{ s}^{-1} \quad (1450\text{--}3370 \text{ K}) \quad (\text{Ref. 11}), \quad (22)$$

and

$$k_1 = 2.64 \times 10^{-7} (T/\text{K})^{-0.927} \exp(-8493 \text{ K}/T) \text{ cm}^3 \text{ molecule}^{-1} \text{ s}^{-1} \quad (1050\text{--}2700 \text{ K}) \quad (\text{Ref. 12}). \quad (23)$$

All of the recent high-temperature experimental data agree with one another and with the present LP-ST results below  $\sim 2000 \text{ K}$ ; however, above  $2000 \text{ K}$  the spread in the values increases to about a factor of 2 as temperature increases to  $2500 \text{ K}$ . The inclusion of the present work changes the situation very little since the agreement with the FP-ST results<sup>10</sup> is so good. The new results do, however, extend the region of temperature overlap significantly. The level of agreement is illustrated in Fig. 5 where the present result is at most  $\sim 19\%$  higher at  $1100 \text{ K}$  than Eqs. (19), (21), (22), and (23) and is within  $\pm 30\%$  of Eqs. (19), (20), (22), and (23) at  $2000 \text{ K}$ . This is well within the combined errors of the present and earlier investigations. The present result agrees best with the data of Masten, Hanson, and Bowman.<sup>11</sup> However, it does not give any information regarding the rate behavior above  $2055 \text{ K}$ . Hence, the factor of 2 spread of values for reaction (1) remains in the database.

Schott<sup>41</sup> recently addressed the continuing spread of values in the rate constants for reaction (1). He suggested an inverse reactant density dependence in the derived  $k_1$  values and included the recent  $\text{H}_2$  oxidation studies,<sup>7-9, 11, 12</sup> his earlier study,<sup>6</sup> and an earlier study by Meyerson and Watt<sup>33</sup> in his correlation. However, the mechanisms and rate constants used in the derivation of  $k_1$  in these studies are not the same. This suggests that other correlations might be possible that involve the kinetics. For example, we note that the rates of initiation vary by about a factor of 3 in the three latest studies. Though all workers have carefully considered the effect of initiation, it is true that at some temperature where the rates of initiation,  $\text{H}_2 + \text{O}_2 \rightarrow \text{HO}_2 + \text{H}$  and the concurrent thermal decompositions of both  $\text{H}_2$  and  $\text{O}_2$ , become comparable to reaction (1), the overall chain center concentration profiles will become strongly dependent on initiation.

The present results for  $k_2$  are the first direct measurements to be reported at high temperature. However, these results can be compared to the earlier indirect  $\text{D}_2$  oxidation results that are listed in Table III. Kurzius and Boudart<sup>13</sup> estimated  $k_2$  from explosion limit studies between  $800$  and  $1000 \text{ K}$ , and their estimate is only  $30\%$ – $40\%$  lower than Eq. (14). Comparison with their results for  $k_1$  from similar  $\text{H}_2/\text{O}_2$  studies gave an isotope effect,  $k_{\text{H}}/k_{\text{D}}$ , of  $0.84$  and  $0.99$  at  $800$  and  $1000 \text{ K}$ , respectively. A shock-tube investigation of the  $\text{D}_2/\text{O}_2$  system by Appel and Appleton<sup>14</sup> yielded values for  $k_2$  that are  $18\%$  lower at  $1700 \text{ K}$  and  $80\%$  higher at  $3100 \text{ K}$  than calculated by Eq. (14). In another shock-tube study by Chiang and Skinner,<sup>15</sup> both the  $\text{H}_2/\text{O}_2$  and  $\text{D}_2/\text{O}_2$  systems were investigated. These authors inferred very low values for  $k_2$  and therefore suggested an isotope effect of  $4.0$ – $5.3$  for the temperature range,  $1000$ – $2200 \text{ K}$ . Subsequently, Pamidimukkala and Skinner<sup>16</sup> repeated the study between  $1000$  and  $2500 \text{ K}$  and found an isotope effect

ranging from  $1.2$  to  $1.7$ . These indirect results are to be compared to the present  $k_{\text{H}}/k_{\text{D}}$  value of  $1.10 \pm 0.36$  for the entire temperature range,  $1085$ – $2278 \text{ K}$ . Within experimental error, there is agreement on the isotope effect from the present and these two earlier studies.<sup>13, 16</sup>

The present results have implications with regard to two related theoretical issues. The first issue is whether the theoretical predictions of  $k_1$  agree with experimental measurements. Since there is only a factor of 3 change in the rate constant for the back reaction,  $k_{-1}$ , over the temperature range,  $300$  to  $\sim 2500 \text{ K}$ , the transformed data substantially expand the differences and therefore illustrate the level of agreement. Accordingly, the  $k_{-1}$  result in Eq. (17), is plotted in Fig. 6 along with the lower-temperature direct results by Lewis and Watson<sup>42</sup> and Howard and Smith.<sup>43</sup> All recent theoretical calculations of  $k_{-1}$ , with the exception of Rai and Truhlar,<sup>20</sup> are also shown for comparison purposes. The earlier methods<sup>17, 18, 20</sup> used the Melius–Blint potential-energy surface;<sup>44</sup> however, it has subsequently been shown that this surface does not asymptotically approach a realistic quadrupole–dipole dependence at large separations. Even so, the quasiclassical trajectory calculations of Miller<sup>17</sup> clearly do not disagree with the data.

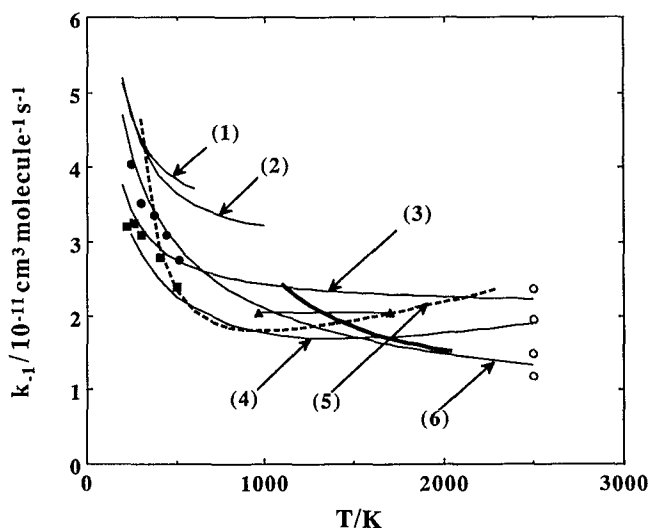


FIG. 6. Experimental and theoretical rate constants for the reverse reaction,  $\text{O} + \text{OH} \rightarrow \text{H} + \text{O}_2$ . Experimental results: bold line, this work; solid circles, Howard and Smith (Ref. 43); solid squares, Lewis and Watson (Ref. 42); solid triangles, Pirraglia *et al.* (Ref. 10); open circles, the recent experimental results at  $2500 \text{ K}$  [from top to bottom: Frank and Just (Ref. 7); Fujii and Shin (Ref. 8); Masten, Hanson, and Bowman (Ref. 11); and Yuan *et al.* (Ref. 12)]. Theoretical results: (1) Clary and Werner (Ref. 21); (2) Graff and Wagner (Ref. 22); (3) Troe (Ref. 19); (4) Pastrana *et al.* (Ref. 23); (5) CTST calculation (see text); (6) Miller (Ref. 17).

The potential-energy surface has been carefully considered by several other workers with the intent being to understand electronic contributions and also the long-range part of the surface, particularly as O departs from OH.<sup>21-24</sup> In the present work we have used the most recent DMBE IV potential surface of Pastrana and co-workers<sup>23</sup> in a conventional transition-state theory (CTST) calculation. The transition state was chosen along the minimum-energy path at the intermediate configuration between the hydrogen-bonded OH–O and the covalently bonded HO<sub>2</sub> species. Pastrana and co-workers<sup>23</sup> have given the configuration and energy relative to separated OH and O ( $V^\ddagger = -1.632$  kcal mol<sup>-1</sup>,  $R_{\text{OH}} = 0.963$  Å,  $R_{\text{OO}} = 2.690$  Å, and  $\angle\text{HOO} = 40.2^\circ$ ). With these values, the assumption that the OH symmetrical stretching frequency is unchanged from the OH radical, and the assumption that the bending frequency is 400 cm<sup>-1</sup> (i.e.,  $\sim 0.4$  of that in HO<sub>2</sub>), the CTST calculation was carried out, and the line that is labeled (5) in Fig. 6 was obtained. The conclusion is that with a variety of surfaces and methods, the theoretical calculations with or without dynamical or statistical recrossing can be made to agree with the data within experimental error. To illustrate this point, the range of uncertainties implied by the recent results on  $k_1$  (Refs. 7, 8, 11, and 12) are shown at 2500 K in Fig. 6 by the open circles. The rate behavior at room temperature is apparently accurate to within  $\sim \pm 10\%$ ,<sup>42,43</sup> and at  $\sim 1100$  K it is probably accurate to within  $\pm 20\%$ ; however, as temperature increases to 2500 K, the error increases to  $\sim \pm 40\%$ . The extent of recrossing has been estimated<sup>17,23</sup> to increase by about a factor of 2 as temperature increases from room temperature to flame temperatures, and this is nearly the same magnitude as the experimental uncertainty. Therefore, the thermal rate data, as they now stand, cannot be used as evidence for the existence of the phenomenon of recrossing.

The second issue is whether the presently measured isotope effect is theoretically sensible. We note that Miller's quasiclassical trajectory theoretical calculations on both  $\text{H} + \text{O}_2$  (Ref. 17) and  $\text{D} + \text{O}_2$ ,<sup>18</sup> when transformed to the back reactions with Eqs. (15) and (16), give a nearly constant isotope effect of  $\sim 1.5$  for back reaction over the entire temperature range of the present study. For  $1100 < T < 2200$  K, the transformed Eqs. (17) and (18) give values between 1.5 and 1.2 with  $\sim \pm 36\%$  error at the one-standard-deviation level. The OD + O CTST calculation with the bending frequency taken to be 283 cm<sup>-1</sup> predicts  $k_{\text{H}}/k_{\text{D}} = 0.99$  over the same temperature range. Hence, neither the present experimental value nor those of both Kurzius and Boudart<sup>13</sup> and Pamidimukkala and Skinner<sup>16</sup> disagree with theory.

*Note added in proof:* Since this manuscript was completed there have been two significant developments concerning the  $\text{H} + \text{O}_2$  and  $\text{D} + \text{O}_2$  reactions. One of these developments is experimental<sup>45</sup> and the other is theoretical.<sup>46</sup>

Du and Hessler<sup>45</sup> have completed a shock tube study of H<sub>2</sub> oxidation with the tunable-laser flash-absorption technique in which OH-radical profiles have been quantitatively monitored. The experiments have been performed in the high temperature range, 2000 to 5300 K. The reason for concentrating on this range was to answer the question as to

whether the  $A$  factor has negative or positive  $T$  dependence as suggested by some of the most recent results.<sup>9,12</sup> These new results, when combined with the present and other studies,<sup>10,11</sup> have supplied data for evaluating the rate behavior over the temperature range, 960 to 5300 K. The result (95% confidence) is,

$$k_1 = (1.62 \pm 0.12) \times 10^{-10} \times \exp(-7474 \pm 122 \text{ K}/T) \text{ cm}^3 \text{ molecule}^{-1} \text{ s}^{-1},$$

and shows no evidence for a  $T$ -dependent  $A$  factor. This result and the present data both agree best with the expression of Masten *et al.*, Eq. (22).<sup>11</sup>

For the temperature range, 1000 to 3000 K, Varandas and co-workers<sup>46</sup> have completed new calculations with the DMBE IV potential energy surface of Pastrana *et al.*<sup>23</sup> as the basis. Three methods have been used: (1) usual quasiclassical trajectory calculations (QCT),<sup>17</sup> (2) quasiclassical trajectory-quantum mechanical threshold calculations (QMT), and quasiclassical trajectory-internal energy-quantum mechanical threshold calculations (IEQMT). Equilibrium constants have also been evaluated. The latter two methods account for zero-point energy effects in different ways. The QMT method appears to agree best with the Du and Hessler result.<sup>45</sup> Also, above 1750 K, the prediction for  $k_{-1}$  is essentially constant at  $\sim 1.5 \times 10^{-11}$  cm<sup>3</sup> molecule<sup>-1</sup> s<sup>-1</sup> with an estimated calculational error of  $\sim 10\%$ . This result is the same as that implied by the experimental conclusion of Du and Hessler within calculational and experimental errors. Since the successful theoretical model incorporated recrossing as an essential feature, such a phenomenon is now likely to exist for this interaction.

Varandas and co-workers<sup>46</sup> have additionally performed quasiclassical trajectory calculations on the  $\text{D} + \text{O}_2$  reaction, and their QMT results agree with the present findings within combined errors. They also predict QMT values for the isotope effect,  $k_1/k_2$ , of 0.75, 0.88, and 1.06 for 1000, 1750, and 2500 K, respectively. Since the calculated  $k_1/k_2$  values are accurate to  $\sim 15\%$ ,<sup>46</sup> these results are not contradicting the experimental inferences from the present study. Hence, the present finding, that the isotope effect is  $1.10 \pm 0.39$ , now has a more firm theoretical corroboration.

## ACKNOWLEDGMENTS

The authors wish to thank Dr. A. F. Wagner and Dr. J. P. Hessler for a thorough reading of the manuscript and helpful suggestions. This work was supported by the U.S. Department of Energy, Office of Basic Energy Sciences, Division of Chemical Sciences, under Contract No. W-31-109-Eng-38.

<sup>1</sup>J. N. Bradley, *Flame and Combustion Phenomena* (Methuen, London, 1969), and references therein.

<sup>2</sup>C. K. Westbrook and F. L. Dryer, *Prog. Energy Combust. Sci.* **10**, 1 (1984), and references therein.

<sup>3</sup>D. L. Baulch, D. D. Drysdale, D. G. Horne, and A. C. Lloyd, *Evaluated Data for High Temperature Reactions* (Butterworths, London, 1972), Vol. 1; D. L. Baulch, R. A. Cox, P. J. Crutzen, R. F. Hampson, J. A. Kerr, and R. T. Watson, *J. Phys. Chem. Ref. Data* **11**, 327 (1982).

<sup>4</sup>N. Cohen and K. R. Westberg, *J. Phys. Chem. Ref. Data* **12**, 531 (1983), and references therein.

<sup>5</sup>J. Warnatz, *Combustion Chemistry*, edited by W. C. Gardiner, Jr. (Springer-Verlag, New York, 1984), and references therein.

- <sup>6</sup>G. L. Schott, *Combust. Flame* **13**, 357 (1973).
- <sup>7</sup>P. Frank and Th. Just, *Ber. Bunsenges Phys. Chem.* **89**, 181 (1985).
- <sup>8</sup>N. Fujii and K. S. Shin, *Chem. Phys. Lett.* **151**, 461 (1988).
- <sup>9</sup>N. Fujii, T. Sato, H. Miyama, K. S. Shin, and W. C. Gardiner, Jr., *Seventeenth International Symposium on Shock Waves and Shock Tubes*, edited by Y. W. Kim (American Institute of Physics, New York, 1989), p. 456.
- <sup>10</sup>A. N. Pirraglia, J. V. Michael, J. W. Sutherland, and R. B. Klemm, *J. Phys. Chem.* **93**, 282 (1989).
- <sup>11</sup>D. A. Masten, R. K. Hanson, and C. T. Bowman, *J. Phys. Chem.* **94**, 7119 (1990).
- <sup>12</sup>T. Yuan, C. Wang, C. -L. Yu, M. Frenklach, and M. J. Rabinowitz, *J. Phys. Chem.* **95**, 1258 (1991).
- <sup>13</sup>S. C. Kurzius and M. Boudart, *Combust. Flame* **21**, 477 (1969).
- <sup>14</sup>D. Appel and J. P. Appleton, *Fifteenth Symposium (International) on Combustion* (The Combustion Institute, Pittsburgh, 1974), p. 701.
- <sup>15</sup>C. Chiang and G. B. Skinner, *Twelfth International Symposium on Shock Tubes and Waves*, edited by A. Lifshitz and J. Rom (Magnes, Jerusalem, 1980), p. 629.
- <sup>16</sup>K. M. Pamidimukkala and G. B. Skinner, *Thirteenth International Symposium on Shock Waves and Shock Tubes* (SUNY, Albany, 1981), p. 585.
- <sup>17</sup>J. A. Miller, *J. Chem. Phys.* **74**, 5120 (1981); **84**, 6170 (1986).
- <sup>18</sup>J. A. Miller, *J. Chem. Phys.* **75**, 5349 (1981).
- <sup>19</sup>C. J. Cobos, H. Hippler, and J. Troe, *J. Phys. Chem.* **89**, 342 (1985); J. Troe, *ibid.* **90**, 3485 (1986); J. Troe, *Twenty-Second Symposium (International) on Combustion* (The Combustion Institute, Pittsburgh, 1988), p. 843.
- <sup>20</sup>S. N. Rai and D. G. Truhlar, *J. Chem. Phys.* **79**, 6046 (1983).
- <sup>21</sup>D. C. Clary and H. J. Werner, *Chem. Phys. Lett.* **112**, 346 (1984).
- <sup>22</sup>M. M. Graff and A. F. Wagner, *J. Chem. Phys.* **92**, 2423 (1990).
- <sup>23</sup>A. J. C. Varandas, *J. Mol. Struct. Theochem.* **166**, 59 (1988); A. J. C. Varandas, J. Brandao, and L. A. M. Quintales, *J. Phys. Chem.* **92**, 3732 (1988); L. A. M. Quintales, A. J. C. Varandas, and J. M. Alvarino, *J. Phys. Chem.* **92**, 4552 (1988); M. R. Pastrana, L. A. M. Quintales, J. Brandao, and A. J. C. Varandas, *J. Phys. Chem.* **94**, 8073 (1990).
- <sup>24</sup>J. Davidsson and G. Nyman, *Chem. Phys.* **125**, 171 (1988); *J. Chem. Phys.* **92**, 2407 (1990); G. Nyman and J. Davidsson, *ibid.* **92**, 2415 (1990).
- <sup>25</sup>D. F. Davidson, A. Y. Chang, and R. K. Hanson, *Twenty-Second Symposium (International) on Combustion* (The Combustion Institute, Pittsburgh, 1988), p. 1877.
- <sup>26</sup>K. S. Shin and J. V. Michael, *J. Phys. Chem.* (submitted).
- <sup>27</sup>G. Burns and D. F. Hornig, *Can. J. Chem.* **38**, 1702 (1960); J. Ernst, H. Gg. Wagner, and R. Zellner, *Ber. Bunsenges. Phys. Chem.* **82**, 409 (1978); K. J. Niemi, H. Gg. Wagner, and R. Zellner, *Z. Phys. Chem. (Frankfurt am Main)* **124**, 155 (1981).
- <sup>28</sup>J. V. Michael, J. W. Sutherland, and R. B. Klemm, *Int. J. Chem. Kin.* **17**, 315 (1985).
- <sup>29</sup>J. V. Michael, *J. Chem. Phys.* **90**, 189 (1989); **92**, 3394 (1990); J. V. Michael and J. R. Fisher, *J. Phys. Chem.* **94**, 3318 (1990).
- <sup>30</sup>J. R. Fisher and J. V. Michael, *J. Phys. Chem.* **94**, 2465 (1990).
- <sup>31</sup>J. V. Michael and J. W. Sutherland, *Int. J. Chem. Kinet.* **18**, 409 (1986).
- <sup>32</sup>J. V. Michael and J. R. Fisher, *Seventeenth International Symposium on Shock Waves and Shock Tubes*, edited by Y. W. Kim (American Institute of Physics, New York, 1989), p. 210.
- <sup>33</sup>A. L. Meyerson, H. M. Thompson, and W. S. Watt, *J. Chem. Phys.* **42**, 3331 (1965); A. L. Meyerson and W. S. Watt, *ibid.* **49**, 425 (1968).
- <sup>34</sup>R. G. Maki, J. V. Michael, and J. W. Sutherland, *J. Phys. Chem.* **89**, 4815 (1985), and references cited therein.
- <sup>35</sup>J. R. Barker and J. V. Michael, *J. Opt. Soc. Am.* **58**, 1615 (1968).
- <sup>36</sup>J. C. Miller and R. J. Gordon, *J. Chem. Phys.* **78**, 3713 (1983).
- <sup>37</sup>K. -J. Hsu, J. L. Durant, and F. Kaufman, *J. Phys. Chem.* **91**, 1985 (1987); K. -J. Hsu, S. M. Anderson, J. L. Durant, and F. Kaufman, *ibid.* **93**, 1018 (1989).
- <sup>38</sup>J. V. Michael and J. W. Sutherland, *J. Phys. Chem.* **92**, 3853 (1988).
- <sup>39</sup>J. V. Michael, J. W. Sutherland, and R. B. Klemm, *J. Phys. Chem.* **90**, 497 (1986).
- <sup>40</sup>M. W. Chase, Jr., J. L. Curnutt, J. R. Downey, Jr., R. A. McDonald, A. N. Syverud, and E. A. Valenzuela, *J. Phys. Chem. Ref. Data* **11**, 695 (1982).
- <sup>41</sup>G. L. Schott, Eastern States Section/The Combustion Institute, 1990 Fall Meeting, Orlando, FL (unpublished).
- <sup>42</sup>R. S. Lewis and R. T. Watson, *J. Phys. Chem.* **84**, 3495 (1980).
- <sup>43</sup>M. J. Howard and I. W. M. Smith, *J. Chem. Soc. Faraday Trans. 2*, **77**, 997 (1981).
- <sup>44</sup>C. F. Melius and R. J. Blint, *Chem. Phys. Lett.* **64**, 183 (1979).
- <sup>45</sup>H. Du and J. P. Hessler, *J. Chem. Phys.* (submitted).
- <sup>46</sup>A. J. C. Varandas, *Studia Chimica* (in press); A. J. C. Varandas, J. Brandão, and M. R. Pastrana (unpublished); A. J. C. Varandas (private communication).